Ecological Modelling 294 (2014) 1–18

Contents lists available at ScienceDirect

Ecological Modelling

journal homepage: www.elsevier.com/locate/ecolmodel

A generalized optimization model of microbially driven aquatic biogeochemistry based on thermodynamic, kinetic, and stoichiometric ecological theory

R.A. Payn [a,b,*], A.M. Helton [c,d], G.C. Poole [a,b,e], C. Izurieta [b,e], A.J. Burgin [f], E.S. Bernhardt [c]

[a] Department of Land Resources & Environmental Sciences, Montana State University, PO Box 173120, Bozeman, MT 59717-3120, USA
[b] Montana Institute on Ecosystems, Montana University System, PO Box 173490, Bozeman, MT 59717, USA
[c] Biology Department, Duke University, Box 90338, Durham, NC 27708, USA
[d] Department of Natural Resources & the Environment and the Center for Environmental Sciences and Engineering, University of Connecticut, 1376 Storrs Road, Unit 4087, Storrs, CT 06269-4087, USA
[e] Computer Science Department, Montana State University, PO Box 173880, Bozeman, MT 59717-3880, USA
[f] School of Natural Resources, University of Nebraska – Lincoln, 3310 Holdrege Street, Lincoln, NE 68583-0961, USA

ARTICLE INFO

Article history:
Received 6 June 2014
Received in revised form 6 September 2014
Accepted 8 September 2014
Available online 27 September 2014

Keywords:
Microbial ecosystem
Aquatic ecosystem
Biogeochemistry
Thermodynamic ecology
Stoichiometry
Ecosystem modeling

ABSTRACT

We have developed a mechanistic model of aquatic microbial metabolism and growth, where we apply fundamental ecological theory to simulate the simultaneous influence of multiple potential metabolic reactions on system biogeochemistry. Software design was based on an anticipated cycle of adaptive hypothesis testing, requiring that the model implementation be highly modular, quickly extensible, and easily coupled with hydrologic models in a shared state space. Model testing scenarios were designed to assess the potential for competition over dissolved organic carbon, oxygen, and inorganic nitrogen in simulated batch reactors. Test results demonstrated that the model appropriately weights metabolic processes according to the amount of chemical energy available in the associated biochemical reactions, and results also demonstrated how simulated carbon, nitrogen, and sulfur dynamics were influenced by simultaneous microbial competition for multiple resources. This effort contributes an approach to generalized modeling of microbial metabolism that will be useful for a theoretically and mechanistically principled approach to biogeochemical analysis.

1. Introduction

Aquatic ecosystems are currently subject to complex changes in external forcing due to changes in land use (Allan, 2004) and climate (Poff et al., 2002). In light of these multivariate changes, empirical data and assumptions of temporal stationarity (in the sense of Milly et al., 2008) are an insufficient basis for understanding the potential biogeochemical trajectories of these ecosystems. Furthermore, empirical work alone may reveal little about feedback effects (Stone and Weisburd, 1992; Singh et al., 2010) that may ultimately cause non-linear or discontinuous system behavior. Therefore, mechanistic simulation models of microbial metabolism are critical to understand the potential changes in aquatic biogeochemical cycles that may emerge from novel and dynamic mixtures of available metabolic reactants.

Use of thermodynamic theory in biogeochemical models relies on a non-equilibrium perspective (Schrödinger, 1944) of microbial metabolism. More specifically, accumulation of microbial biomass requires that the system must be far from equilibrium (Jørgensen et al., 1992), conservative of mass and energy (Patten et al., 1997), dissipative in the generation of entropy from available energy (Straškraba et al., 1999), and open to external sources and sinks of energy and matter (Jørgensen et al., 1999). This perspective assumes that microbial metabolism is inherently adapted to a state of disequilibrium, because the structure and function of a microbial assemblage is sustained by exergy (energy capable of work) provided by external factors (e.g., incoming solar or chemical energy). Starting from this premise, the non-equilibrium thermodynamic theory of ecology has led to several proposed goal

* Corresponding author. Tel.: +1 4069947197.
E-mail addresses: rpayn@montana.edu (R.A. Payn), ashley.helton@uconn.edu (A.M. Helton), gpoole@montana.edu (G.C. Poole), clemente.izurieta@cs.montana.edu (C. Izurieta), aburgin2@unl.edu (A.J. Burgin), emily.bernhardt@duke.edu (E.S. Bernhardt).

http://dx.doi.org/10.1016/j.ecolmodel.2014.09.003

functions that lead to the emergence of system complexity from imposed exergy sources (Fath et al., 2001). These goal functions include: maximum dissipation potential (Schneider and Kay, 1994), maximum exergy storage (Jørgensen et al., 2000), and maximum entropy production (Vallino, 2010). A model that maximizes microbial biomass using the available chemical potential is generally consistent with these goal functions, and provides a method by which thermodynamic ecological theory can be applied to (and tested by) field or lab studies of biogeochemical dynamics driven by microbial metabolism (Jessup et al., 2004; Prosser et al., 2007; Hall et al., 2011).

A non-equilibrium perspective alone would suggest that an appropriate metabolic model would be strictly rate-limited by kinetics, as opposed to equilibrium-limited, and the potential for kinetic drivers to control rates of metabolic activity is, indeed, an important consideration for any biochemical system. However, a generalized metabolic model also requires simulation of the effects of microbial competition for resources (Kalyuzhnyi and Fedorovich, 1998; Cherif and Loreau, 2007; van de Leemput et al., 2011). For example, a strictly rate-limited model for each heterotrophic metabolic reaction would predict that all terminal electron acceptors (TEAs) used for oxidizing dissolved organic carbon (DOC) would be consumed simultaneously, according to the relative magnitude of each predicted reaction rate. But in reality, exclusive separation of TEA consumption is commonly observed over space and time when chemical energy in the form of DOC is limiting (Hedin et al., 1998; Tesoriero et al., 2000; Zarnetske et al., 2011). This separation is typically attributed to competition for DOC among microbes capable of different heterotrophic metabolic pathways (e.g., aerobic respiration, denitrification, or sulfate reduction), and thermodynamic principles predict that microbes capable of higher energy-yielding metabolic reactions outcompete those capable of lower yielding reactions (Hedin et al., 1998). Therefore, we suggest that an effective generalized model of biogeochemistry should account for the potential occurrence of both kinetic and thermodynamic drivers (Jin and Bethke, 2003). Our use of the term “thermodynamic driver” does not refer to the more conventional definition of a system limited by reaching equilibrium, which would require death or dormancy for all life inhabiting that system (Schrödinger, 1944). Here, thermodynamic driver refers to an optimization algorithm that selects the metabolic processes that use the highest available energy yields from the available biochemical reactions.

The requirements for computer software supporting both our current and future modeling efforts are driven by the scientific needs of an adaptive hypothesis testing cycle. To initiate the cycle, a modular model that can be easily extended is constructed with a foundational set of hypotheses representing maximum parsimony. We define maximum parsimony as the simplest mechanistic explanation for a given set of observations. The initial model is configured and parameterized to simulate behavior of a real study system under a given experimental scenario. Comparison of the simulation with observations from the study system suggest how hypotheses encapsulated within the model need to be adapted to explain residual error. To maintain parsimony, complexity is added to the model only when it explains a statistically significant portion of the residual error. Further statistical analyses with the adapted model can then be used to suggest optimal designs for future laboratory or field experimentation, thus starting the next iteration of the cycle.

Here, we present a model framework designed to initiate this cyclic and adaptive approach for an assessment of biogeochemical trajectories of aquatic microbial ecosystems. Our objective was to develop an extensible biogeochemical modeling tool based on the metabolism of aquatic microbial assemblages, where the application of thermodynamic, kinetic, and stoichiometric theory is generalized to a level appropriate for simulating whole-system solute dynamics. We demonstrate a version of the model that incorporates the minimum conceptual complexity (or maximum parsimony) necessary to simulate system behavior that is consistent with modern thermodynamic and stoichiometric interpretations of microbially driven biogeochemistry.

2. Model description

Many models of microbial metabolism and growth have been based on some combination of thermodynamic, stoichiometric, and kinetic principles (Menkel and Knights, 1995; Vallino et al., 1996; Jin and Bethke, 2003; Franklin et al., 2011; van de Leemput et al., 2011). We build on these examples with a model implementation that has sufficient extensibility to be used in hypothesis testing against data from the typical aquatic ecosystem field or lab study. We designed a model where the suite of potential biogeochemical reactions was configurable at run time, allowing the researcher to define the appropriate simulation for a particular system or particular hypothesis of interest (similar to Flynn (2001)). The code was implemented in a highly modular, object-oriented framework for the purposes of (1) facilitating implementation of code to address new hypotheses that may arise from continued field and lab studies, and (2) allowing future integration with a hydrologic model to simulate physical transport of solutes.

We implemented the microbial ecosystem model using the Network Exchange Objects (NEO) modeling framework (Izurieta et al., 2012), coded in Java (v. 1.7, Oracle Corporation, Redwood Shores, California, USA). Critical NEO features include: (1) a shared name space for state variables within node and link objects based on a network-based data structure and (2) a dependency manager that automatically determines the appropriate execution order for calculating the new values for each state during a simulation time step. In this fashion, the NEO framework is designed to integrate the results of a collection of relatively simple individual calculations, in order to simulate the relatively complicated emergent interactions that may occur in the ecosystem.

We defined a functional unit of the microbial ecosystem with three nodes, where each node represents a particular physical location or conceptual structural component of the ecosystem (Fig. 1). The characteristics of these nodes are similar to model compartments proposed by Franklin et al. (2011), though less detailed in their ability to track variation of biomass stoichiometry. The nodes track the storage of compounds in various locations or forms, including: (1) the aqueous node, which tracks the amount and concentration of each simulated compound in the aqueous environment; (2) the biologically available node, which tracks the amounts of compounds that are in immediate proximity with enzymes driving metabolic processes; and (3) the biomass node, which tracks the amounts of elements that comprise living biomass (in this case, C and N).

NEO code is highly modular, where classes are organized within specific “behavior packages” that each define how a specific compound will behave in a given type of node or link. Model boundary conditions are implemented as one-sided links (henceforth called “boundary links”) that conceptually tie a single node to the exterior of the model domain. In this fashion, we describe how compounds and elements are moved and transformed within the microbial ecosystem by describing the general “behavior” of compounds in a given two-sided link between nodes, and we define the relationship between the ecosystem and external entities (e.g., driving data, compound source/sinks, etc.) by describing the behavior of compounds in one-sided boundary links connected to a single node.

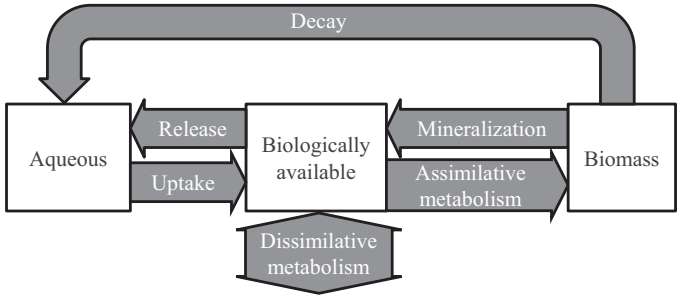

Fig. 1. Flux network for a functional unit of the microbial ecosystem model. Boxes are nodes that track storage of compounds, and arrows are links that control the flux of compounds between nodes.

2.1. Simulation of uptake kinetic behavior

Potential biological use of aqueous compounds is first simulated as an uptake calculation between the aqueous node and the biologically available node ("Uptake" in Fig. 1). We apply kinetic theory to determine availability of compounds as a function of the aqueous concentration, which is a common approach to translating concepts from bench-top chemistry experiments to whole-system behavior (Dodds et al., 2002; Ribot et al., 2013). For this effort, we applied an adaptation of the Monod saturating function.

$$U_X = \frac{C_X U_{XB,max}}{C_X + C_{X,half}} \quad (1)$$

where U_X is the uptake rate of compound X ((mole X) time^{-1}); $U_{XB,max}$ is the maximum uptake rate of compound X relative to moles of carbon in biomass ((mole X) time^{-1} (mole C)$^{-1}$); $C_{X,half}$ is the concentration of compound X at which half the maximum uptake occurs ((mole X) length^{-3}); C_X is the aqueous concentration of compound X ((mole X) length^{-3}); and B_t is the standing stock of microbial biomass at time t (mole C).

For the purposes of this model, the concept of "biologically available" implies that a compound must be physically "taken up" from relatively free aqueous form into proximity of the enzymes necessary for metabolic reactions to occur (either intra- or extracellular). Simulating uptake as a single saturating kinetic function of concentration and biomass is a simplification, because the rate at which uptake actually occurs is potentially determined by a multitude of both physical processes (e.g., diffusion limitation) and biological processes (e.g., biochemical kinetic limitation). This simplification is necessary for our purposes because the data needed to simulate these processes independently (with any confidence) is not commonly available in even the most meticulous biogeochemical surveys. Eq. (1) ultimately determines the biological availability of compounds to a metabolic optimization (see Section 2.2), such that its calculation will only result in effective reactive rate limitation when simulated uptake is less than the optimized thermodynamic demand.

2.2. Thermodynamic and stoichiometric optimization of metabolic variables

As a result of uptake, the abundances of various electron donors and acceptors in the biologically available node define the chemical exergy that supports the maintenance and growth of the microbial assemblage. An application of non-equilibrium thermodynamic theory to microbial ecology suggests that a microbial assemblage will optimize its structure using available exergy, in order to meet a thermodynamic goal (Fath et al., 2001), such as maximize exergy storage (Jørgensen et al., 2000), maximize entropy production (Vallino, 2010), or maximize dissipation (Schneider and Kay, 1994). Quantitative application of this theory requires definition of assemblage structure and available exergy as measurable properties of the system, and then definition of how that structure is optimized relative to the available exergy. In the interest of maximum parsimony, our goal was to quantify these properties with a minimum number of variables, and still generate predictions of complex biogeochemical patterns that are consistent with observations that motivated the underlying theory.

Structure of microbial assemblages has been viewed from many perspectives, as reviewed by Treseder et al. (2012). We chose to start with the most parsimonious definition, where optimized assemblage structure is represented simply by maximizing the total quantity of carbon in living biomass. Simulation of microbial biomass was divided according to metabolic assimilation of different carbon sources. Thus, the optimization separately tracks the biomass and metabolic demands of autotrophs, heterotrophs, and methanotrophs. We refer to this as the more generalized "carbon source specific model", in order to distinguish it from the more detailed "species specific" or "gene specific" models that use more complex characterizations of microbial structure. Regardless of the degree to which simulation of the microbial assemblage is segregated, the set of thermodynamic and stoichiometric constraints on each group can be generalized in a common linear mathematic form, which can subsequently be optimized for maintaining maximum total biomass.

In an aqueous biogeochemical system that is not exposed to sunlight, the available exergy of interest is based on the chemical potential present in dissolved reactants. More specifically, exergy is available in the dissolved chemical compounds that have potential to be used in exergonic metabolic redox reactions facilitated by microbial enzymatic activity. The exergy represented by each of these potential reactants can be estimated by the established standard free energies of reaction for the associated metabolic redox reaction (Table 1), where occurrences of reactions with more negative free energies result in a larger contribution of exergy to metabolism.

We defined a linear optimization scheme that maximizes the standing stock of microbial biomass based on the availability of metabolic reactants (Fig. 2). Because energy is required for either maintaining or growing the maximized biomass, this inherently results in higher energy yielding metabolic reactions taking precedence over lower energy yielding reactions (Table 1). The optimization was designed to operate over each model time step (Δt), during which the biomass remaining at the end of the time step $B_{t+\Delta t}$ is maximized as a function of the biomass and reactants available at the beginning of the time step (B_t and X_t). The optimization scheme arrives at a unique solution using a suite of linear constraints defined by conservation of energy and mass within the ecosystem.

The fundamental constraining linear equation was based on conservation of energy, which requires that energy supplied by

Table 1
List of metabolic redox reactions currently supported by the model, and their energy yields as estimated from standard free energies of reaction (Stumm and Morgan, 1996). Energy yields are provided as per mole of reaction, using the stoichiometry of the reactions as presented in the table. For easier comparison among the yields critical to the optimization, heterotrophic reactions have all been balanced to a common amount of acetate, and autotrophic and methanotrophic reactions have all been balanced to a common amount of dioxygen. End-to-end nitrification and denitrification reactions are provided for reference, but are not currently used in the optimization scheme.

Metabolic process	Reaction	$E_S = -\Delta G_0'$ (kJ mol^{-1})
Aerobic respiration	$\frac{1}{2}CH_3COOH + O_2 \leftrightarrow CO_2 + H_2O$	437
Denitrification:	$\frac{1}{2}CH_3COOH + \frac{4}{5}NO_3^- + \frac{4}{5}H^+ \leftrightarrow CO_2 + \frac{2}{5}N_2 + \frac{7}{5}H_2O$	410
Nitrate reduction undefined	$\frac{1}{2}CH_3COOH + 2NO_3^- \leftrightarrow CO_2 + 2NO_2^- + H_2O$	288
Nitrite reduction	$\frac{1}{2}CH_3COOH + 2NO_2^- + 2H^+ \leftrightarrow CO_2 + N_2O + 2H_2O$	415
Nitrous oxide reduction	$\frac{1}{2}CH_3COOH + 2N_2O \leftrightarrow CO_2 + 2N_2 + H_2O$	645
Sulfate reduction	$\frac{1}{2}CH_3COOH + \frac{1}{2}SO_4^{-2} + \frac{1}{2}H^+ \leftrightarrow \frac{1}{2}HS^- + CO_2 + H_2O$	38
Methanogenesis	$\frac{1}{2}CH_3COOH \leftrightarrow \frac{1}{2}CO_2 + \frac{1}{2}CH_4$	28
Nitrification:	$O_2 + \frac{1}{2}NH_4^+ \leftrightarrow \frac{1}{2}NO_3^- + H^+ + \frac{1}{2}H_2O$	174
Ammonium oxidation	$O_2 + \frac{2}{3}NH_4^+ \leftrightarrow \frac{2}{3}NO_2^- + \frac{4}{3}H^+ + \frac{2}{3}H_2O$	183
Nitrite oxidation	$O_2 + 2NO_2^- \leftrightarrow 2NO_3^-$	148
Methanotrophy	$O_2 + \frac{1}{2}CH_4 \leftrightarrow \frac{1}{2}CO_2 + H_2O$	409

metabolic reactions (E_S) must be equal to the total energy required by biomass (E_R).

$$E_S = E_R = E_{RM} + E_{RG} \tag{2}$$

where E_{RM} is the energy required for biomass maintenance respiration and E_{RG} is the energy required for biomass growth. The energy required for maintenance respiration is proportional to the standing stock of biomass.

$$E_{RM} = m_M \frac{B_t + B_{t+\Delta t}}{2} \tag{3}$$

where m_M is the energy needed to maintain each mole of carbon in biomass over the optimization time step; and B_t and $B_{t+\Delta t}$ are moles of carbon in biomass at the beginning and at the end of the optimization time step, respectively. Note that this calculation is based on the average biomass over the model time step, which helps prevent lack of convergence of the optimization when resources are scarce and biomass is declining. For the carbon source specific model, the value of m_M was assumed to be the same for autotrophs, methanotrophs, and heterotrophs (B_A,B_M, and B_H).

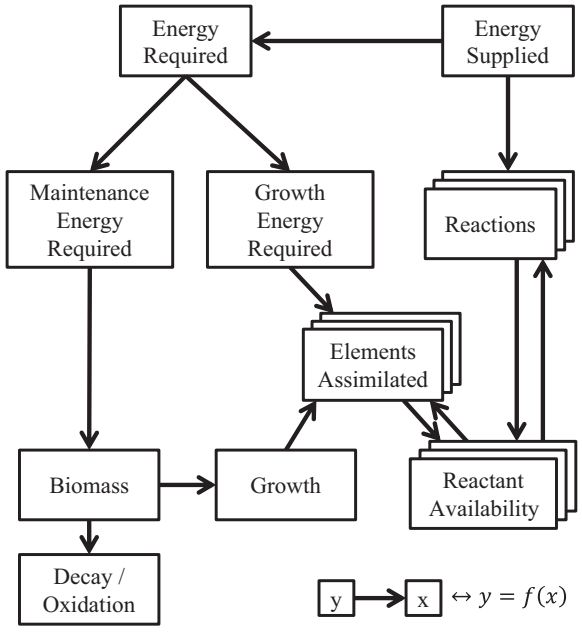

Fig. 2. Variable dependency diagram for the microbial metabolism and growth optimization scheme. Boxes are variables, and arrows indicate dependencies between variables.

The energy required for growth was considered to be proportional to assimilation of elements into biomass.

$$E_{RG} = \sum_{j=1}^{n_G} m_{G,j} G_j \tag{4}$$

where n_G is the number of compounds that can be assimilated into biomass for growth (e.g., carbon and nitrogen sources tracked by the model, Table 2); j is a counter for each compound that may be assimilated; $m_{G,j}$ is the energy needed to assimilate a mole of a necessary element from compound j (e.g., Table 2); and G_j is the moles of compound j assimilated into biomass for growth. For example, the value of m_G for assimilation of carbon varies among autotrophs using inorganic carbon (m_{GA}), methanotrophs using methane (m_{GM}), and heterotrophs using organic carbon (m_{GH}). The energetic cost of carbon fixation from an inorganic form is relatively high, so the energy required for growth of autotrophs (m_{GA}) is higher than the energy required for growth of heterotrophs (m_{GH}) and methanotrophs (m_{GM}). The energy supplied is the sum of free energies of the dissimilative metabolic reactions that occur during the optimization time step (Table 1).

$$E_S = \sum_{i=1}^{n} m_{S,i} E_{S,i} \tag{5}$$

where n is the number of different reactions that may occur during the time step (e.g., number of rows in Table 1); i is a counter that differentiates each type of reaction (e.g., each row in Table 1); $E_{S,i}$ is the energy provided by a given type of dissimilative metabolic reaction for each mole of reactions; and $m_{S,i}$ is the moles of reactions that occur for that type of reaction during the optimization time step. For the current model, three constraints for the energy supplied to autotrophs, heterotrophs, and methanotrophs are implemented (Table 3).

Further linear optimization constraints are necessary to ensure mass conservation of all the compounds tracked by the model. These constraints are based on the stoichiometry of elements in metabolic reactions (Table 1) (Stumm and Morgan, 1996) and the stoichiometry of elements required for growth (e.g., Redfield, 1958). The linear mass balance constraints for stoichiometry take the general form

$$X_{t+\Delta t} \geq 0 \tag{6}$$

$$X_{t+\Delta t} = X_t + \sum_{i=1}^{n} f_{XP,i} m_{S,i} - \sum_{i=1}^{n} f_{XR,i} m_{S,i} - \sum_{j=1}^{n_G} f_{XG,i} G_C \tag{7}$$

where X_t and $X_{t+\Delta t}$ are the biologically available amount of compound X (moles) at the beginning and at the end of an

Table 2
List of model parameter values used for testing.

Variable	Value	Unit	Description	Source
Monod parameters				
$U_{XB,max}$	0.435	mmol-X mmol-C-biomass^{-1} h^{-1}	Maximum uptake rate of compound X normalized to amount of biomass	Average of values for various types of dissolved organic matter from Peil and Gaudy, Jr. (1971)
$C_{X,half}$	2.83	mmol L^{-1}	Concentration of compound X at which half the maximum uptake occurs	Average of values for various types of dissolved organic matter from Peil and Gaudy, Jr. (1971)
Energy demand for maintenance respiration				
E_{RM}	2.83	kJ mol-C-biomass^{-1} h^{-1}	Energy demand for maintenance of biomass	Value at 20 °C from Tijhuiset al. (1993)
Energy demand for assimilation				
m_{GA}	3500	kJ mol-C-growth^{-1}	Energy demand for fixation of carbon (autotrophy)	Heijnen and van Dijken (1992)
m_{GH}	432	kJ mol-C-growth^{-1}	Energy demand for assimilation of organic carbon and nitrogen into living biomass (heterotrophy)	Estimated from empirical relationship in Heijnen and van Dijken (1992)
m_{GM}	1090	kJ mol-C-growth^{-1}	Energy demand for assimilation of methane into living biomass (methanotrophy)	Estimated from empirical relationship in Heijnen and van Dijken (1992)
m_{G,NH_4^+}	31	kJ mol-N-assimilated^{-1}	Energy demand for assimilation of ammonium into living biomass	Based on one ATP half reaction that provides the energy for conversion of ammonium to an amine
m_{G,NO_2^-}	124	kJ mol-N-assimilated^{-1}	Energy demand for assimilation of nitrite into living biomass	Based on the half reactions for generation of 3 NADH used to reduce nitrite (6 e$^-$) and 1 ATP to assimilate resulting ammonium
m_{G,NO_3^-}	155	kJ mol-N-assimilated^{-1}	Energy demand for assimilation of nitrate into living biomass	Based on the half reactions for generation of 4 NADH used to reduce nitrate (8 e$^-$) and 1 ATP to assimilate resulting ammonium

optimization time step, respectively; $f_{XP,i}$ is the stoichiometric factor for compound X in any metabolic reactions where it is a product; $f_{XR,i}$ is the stoichiometric factor for compound X in any metabolic reactions where it is a reactant; $f_{XR,i}$ is the stoichiometric factor for assimilation of compound X relative to carbon assimilated for growth ((mole X) (mole C)$^{-1}$); and G_C is the moles of C assimilated into biomass for growth. The potential interactions of these mass balance constraints can be quite complex, due to the fact that certain compounds (e.g., NO_3^-) are a reactant in some reactions (e.g., denitrification), a product in other reactions (e.g., nitrification), and a source of an element necessary for growth (e.g., assimilatory NO_3^- reduction). Employment of a simultaneous solution scheme for multiple linear equations precludes the need to develop an ordered algorithm to handle this emergent complexity. Thus, the linear optimization scheme is a key to the ease of adding further reactions and compounds to this generalized model.

The final constraint represents the mass balance of carbon assimilated with growth of biomass or released with decay of biomass due to insufficient energy for maintenance.

$$B_{t+\Delta t} = B_t + G_C - D_{IE} \quad (8)$$

where D_{IE} is the moles of carbon (in DOC form) released by decay of biomass due to insufficient energy. As a result of this constraint and the maximization of $B_{t+\Delta t}$ by the optimization scheme, decay only occurs by this mechanism when maintenance energy demands cannot be met by the available chemical energy in potential redox reactions. Carbon released by decay of heterotrophs is immediately used for heterotrophic respiratory processes (within the same optimization time step). In other words, the available DOC for the mass balance in Eq. (7) for heterotrophy includes the carbon released by decay.

Iterated over time, this optimization scheme simulates the dynamics of a microbial assemblage subject to external controls on aqueous reactant availability. When chemical potential is abundant (higher exergy availability), iteration of this optimization scheme results in simulated microbial assemblages with increasing biomass (more ecosystem structure). When chemical potential is depleted (lower exergy availability), simulated biomass in the system will decrease (less ecosystem structure), because resources are insufficient to meet the maintenance respiration energy demand of the microbial standing stock.

The optimization code was implemented in a metabolism sub-processor class within the governing object-oriented microbial ecosystem model (i.e., the NEO model). Methods in the sub-processor class use the Java interface to lp_solve, an open source linear program solver based on the revised simplex method (v. 5.5.2.0, http://lpsolve.sourceforge.net). During each time step, the metabolism sub-processor performs an independent lp_solve optimization, based on initial conditions provided by the uptake calculations and current state of the governing model (see Appendix A). These initial conditions include the amounts of compounds in the biologically available node and the amount of carbon in living biomass. Once the execution of the optimization

Table 3
Examples of the optimization constraints for energy provided by autotrophic, heterotrophic, and methanotrophic metabolic processes. For the values provided, energy supplied (E_S) is are units of kJ (Table 1), and units of number of reactions (m_S) is in moles. For the constraint for energy provided by autotrophic reactions (E_{SA}), subscripts for the m_S variables indicate the energy source. For the constraints for energy provided by heterotrophic (E_{SH}) and methanotrophic (E_{SM}) reactions, subscripts for the m_S variables indicate the terminal electron acceptor.

Carbon source	Constraint for energy supplied
Inorganic (autotrophs)	$E_{SA} = 183m_{SA,NH_4^+} + 148m_{SA,NO_2^-}$
Organic (heterotrophs)	$E_{SH} = 437m_{SH,O_2} + 288m_{SH,NO_3^-} + 415m_{SH,NO_2^-} + 645m_{SH,N_2O} + 38m_{SH,SO_4^-} + 28m_{SH,CO_2}$
Methane (methanotrophs)	$E_{SM} = 409m_{SM,O_2}$

is complete, the variables representing the unique solution are made available to the governing microbial ecosystem model for subsequent flux and mass balance calculations among the 3 nodes. The effects of the flux and mass balance calculations determine the state of the model at the beginning of the next time step.

2.3. Simulation of ecosystem metabolic behavior

The optimized solutions from the metabolism sub-processor provides critical data to the NEO model that simulates changes in microbial ecosystem over time. Model calculations that determine rates of assimilation of compounds into biomass are defined in the link between the biologically available node and the biomass node ("Assimilative metabolism" in Fig. 1). Rates for these assimilative processes are derived from the optimized assimilation term of Eq. (7) from the metabolism sub-processor $-\sum_{j=1}^{n_C} f_{XG,i} G_C$. Model calculations that determine rates of dissimilative metabolic reactions are defined in the boundary link connected to the biologically available node ("Dissimilative metabolism" in Fig. 1). Rates for these processes are derived from the optimized product and reactant terms of Eq. (7) from the metabolism sub-processor $\left(\sum_{i=1}^{n} f_{XP,i} m_{S,i} - \sum_{i=1}^{n} f_{XR,i} m_{S,i}\right)$. Model calculations that determine rates of mineralization of compounds from dissimilative use of dissolved organic matter (e.g., ammonium from respired dissolved organic matter) are also defined in the dissimilative metabolism boundary link. Rates for mineralization from dissolved organic matter (DOM) are based on the stoichiometry of the mineralized element in the biologically available node relative to the respiration of DOC. For example, available DOM with a C:N ratio of 6:1 will produce 1 mole of NH_4^+ for every 6 moles of DOC respired.

Model calculations that determine the total decay of biomass are defined in a link between the biomass node and the aqueous node, representing the movement and transformation of compounds from living biomass directly back to aqueous compounds ("Decay" in Fig. 1). Total decay is calculated as the sum of the decay due to insufficient energy resources (from Eq. (8) for autotrophs and methanotrophs) with the decay due to a constant microbial turnover rate (due to lysis or predation (van Loosdrecht and Henze, 1999)).

$$D_{DOC} = D_{IE} + d_{TO} B_{t+\Delta t} \tag{9}$$

where D_{DOC} is the total amount of DOC generated by decay and d_{TO} is the fraction of remaining biomass that decays per unit time due to microbial turnover. When Eq. (9) is applied to heterotrophs, $D_{IE} = 0$ because any decaying biomass is immediately respired for energy within the same time step (see Section 2.2), and hence it will not return to the aqueous node as DOC. Model calculations that determine rates of mineralization of compounds from respired heterotrophic biomass (i.e., heterotrophic D_{IE}) are defined in the link between the biomass node and the biologically available node ("Mineralization" in Fig. 1). Rates for release of these mineralized compounds to the biologically available node are in proportion to their stoichiometric ratio with biomass C.

After all metabolic changes are calculated for a given time step, any unused or unmodified compounds remaining in the biologically available node are released back to the aqueous node, as if they were never taken up at the beginning of the time step (via "Release" in Fig. 1). This would suggest that the biologically available node is not technically necessary for the current implementation of the model. However, we included the biologically available node in this extensible model because it will become necessary if simulation of uptake of compounds stored for later demands (i.e., luxury uptake) becomes a feature needed in future numerical experiments.

2.4. Model implementation for testing

The current implementation of the model accounts for the following potential metabolic pathways: aerobic respiration of DOC, denitrification, sulfate reduction, acetoclastic methanogenesis, nitrification, and methanotrophy (Table 1). The compounds tracked by the governing model are DOC, dissolved organic nitrogen (DON), dissolved oxygen (DO), nitrate (NO_3^-), sulfate (SO_4^{2-}), methane (CH_4), and ammonium (NH_4^+). Note that this model separates the incremental reactions associated with denitrification and nitrification (Table 1). This allows the incremental species of nitrite (NO_2^-) and nitrous oxide (N_2O) to be available for all processes of dissimilative and assimilative metabolism within the linear optimization calculation, which is a relatively unique feature in nitrogen cycling models. However, these incremental species are tracked only in the biologically available cell and are not subject to release and uptake with the aqueous cell. Thus, the current model does not simulate the kinetic drivers of the denitrification of N_2O or the kinetic drivers of nitrification and denitrification of NO_2^-.

Quality of aqueous DOC is simulated only through the relative amount of aqueous DON, assuming there is no difference in the lability of the various carbon structures among aromatic, aliphatic (with the exception of methane), protein, lipid, and carbohydrate compounds. In the interest of parsimony for this effort, the ratio of C:N in simulated biomass is held constant at the Redfield ratio (Redfield, 1958), and the assimilation of DON is assumed to be proportional to that of DOC according to the DOC:DON ratio in the biologically available node.

2.5. Simulation environment for numerical batch reactor experiments

For initial tests, we required applications of the microbial ecosystem model that simulate and compare the behaviors of multiple independent functional units (i.e., closed systems). This approach to model validation is consistent with the strategy of unit testing (Huizinga and Kolawa, 2007), where the independent behavior of functional units must be validated before simulations of more complex interactions among multiple functional units can be trusted. Furthermore, this reference frame for tests of the microbial ecosystem model is directly analogous to experimental design for laboratory batch reactors, due to the closed system environment being simulated. Therefore, through the remainder of this document, we refer to our application of the model as the batch reactor simulation environment. Primary design constraints for this simulation environment include the ability to define the following properties at run time: (1) initial concentrations of all simulated compounds in the aqueous node and initial carbon and nitrogen in biomass;(2) Monod parameters for every compound simulated in aqueous form and parameters controlling metabolic energy demands and decay; (3) activation or deactivation of particular metabolic reactions; and (4) automatic generation of plots of any state in the model vs. simulated time, where the layouts of graphs are configurable for interpretation of results. The batch reactor simulation environment was coded as a Java application that uses a direct programmers' interface to the NEO microbial ecosystem model.

The simulation environment implementation consists primarily of pre- and post-processors that are executed before and after a given NEO model execution. The pre-processor creates the NEO model input necessary to define the control parameters and the characteristics of the reactors to be simulated by the model. After execution of the pre-processor is complete, the simulation environment executes the governing NEO model, thereby generating output that quantifies the simulated behavior of each configured batch reactor. The post-processor extracts data from

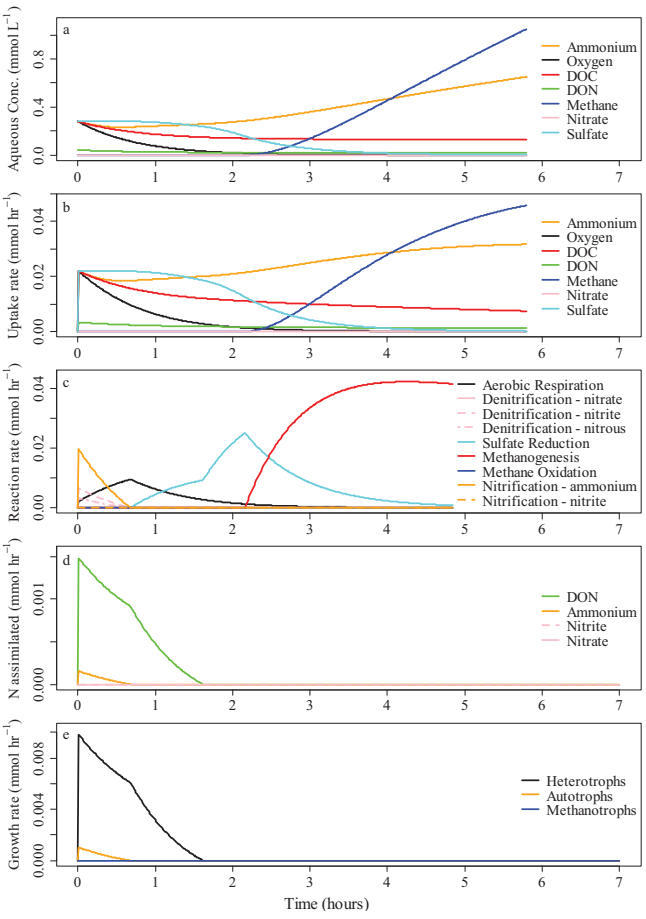

Fig. 3. Example of output from a simulated batch reactor, including (a) aqueous concentrations of simulated compounds, (b) Monod uptake rate of compounds from the aqueous to the biologically available cell, (c) metabolic reaction rate predicted by the optimization scheme, (d) N assimilation rate predicted by the optimization scheme, and (e) biomass growth. This example was taken from simulation 2b.

NEO output into time series tables for each simulated reactor (in space-delimited text files), and automatically generates R scripts (R Core Team, 2012) for visually summarizing model behavior (e.g., Fig. 3, actual graphs from model output have been formatted for publication standards and continuity with text). These tables can also be manually imported into any common data analysis software, such as R, MatLab or Microsoft Excel, for external analysis and visualization. With these features, the environment is designed to facilitate simulations of sets of batch reactors that produce output mimicking typical results from a controlled laboratory bench-top experiment.

3. Model configuration and testing

Fundamental tests of batch reactor simulations were designed to ensure that potentially complex interactions among the multiple metabolic pathways behaved consistently with observations that motivate the underlying thermodynamic theory. Batch reactor simulations were configured to demonstrate the progression of metabolic reactions from the highest to lowest energy yield, as the total chemical potential of solutes was depleted in the closed system simulations. Definition of these simulations required quantifying parameters for the energy yield of reactions, the energy demands of the system, and the Monod kinetics governing availability of compounds to the optimization. Furthermore, each simulation required initial conditions for biomass and compound concentrations that would provide a clear illustration of the progression of simulated reactions occurring in each reactor. As described below, parameters were derived from the literature and initial conditions were taken from case studies and simple hypothetical scenarios.

All simulations were executed with a time step of 0.01 h. This is very short compared to the time scale of the changes occurring in model state variables, and thus minimizes the potential for the selection of the time step to influence our conclusions. As with any finite approximation model, further sensitivity analysis with the time step would be necessary to minimize model run times without affecting results.

3.1. Model parameters

Energy yields of dissimilative metabolic reactions (E_S) were based on the standard free energies of reaction (based on per mole of reactions with the stoichiometry presented in Table 1). In the absence of enzymatic inhibition and under natural conditions, the simulated reactions all have relatively high equilibrium constants and can generally be assumed to proceed to completion. Therefore, for our current purposes, the standard free energy is a reasonable first order approximation of energy yield. Accurate estimates of the actual free energies of reaction would require that we know how concentrations of solutes in proximity to biochemical enzymes (e.g., in the biologically available node) are related to uptake processes, biofilm or cell volume, and aqueous concentrations. This level of process complexity is outside the scope of our current effort.

The energy required for maintenance respiration was assumed to be a function only of temperature, and not a function of the microbial species or active metabolic pathways (Tijhuis et al., 1993). Simulated batch reactors were assumed to be incubated at room temperature (20 °C), and E_{RM} was thus set to 2.83 kJ mol-C-biomass^{-1} h^{-1} (Table 2) according to empirical relationships derived by Tijhuis et al., (1993).

The energy required for growth in the current model is the sum of the energy required for C and N assimilation. The energy required for C assimilation is determined by the molecular structure of the C source and the degree of reduction of C in those molecules (Heijnen and van Dijken, 1992). We used an empirical relationship derived by Heijnen and van Dijken (1992) to estimate the energy requirements for growth of heterotrophs (m_{GH}) and methanotrophs (m_{GM}). We assumed that DOC was relatively labile and had an energetic cost of heterotrophic assimilation similar to that of acetate (number of C atoms in the source molecule = 2 and degree of C reduction = 4). Thus, the energy requirement for heterotrophic growth was m_{GH} = 432 kJ mol-C-growth^{-1}. While this assumption is suitable for our initial model testing, accuracy of simulations compared to real carbon sources would likely require a higher cost of DOC assimilation. We also assumed that the DON associated with assimilated DOC was available for heterotrophic growth at no additional energetic cost. This assumption may be unrealistic in some scenarios, but it is consistent with the idea that most of the metabolic work necessary to assimilate DON is completed by the degradation of DOM molecules necessary for C assimilation. In the current model, heterotrophs also have potential to assimilate inorganic N if the DON available for assimilation is insufficient for potential growth.

For methanotrophic growth, the number of C atoms in methane is 1 and the degree of C reduction is 8, resulting in an energy requirement of m_{GM} = 1090 kJ mol-C-growth^{-1} (Heijnen and van Dijken, 1992). Also based on the findings of Heijnen and van Dijken (1992), we assumed the cost of carbon fixation and assimilation by autotrophs to be m_{GA} = 3500 kJ mol-C-growth^{-1}. In the current model, both methanotrophs and autotrophs must assimilate inorganic N for growth.

Variability in the cost of inorganic N assimilation among different nitrogenous compounds (e.g., NH_4^+, NO_2^-, NO_3^-) is important in determining which form of N is preferred under a given simulation scenario. Thus, the relative costs of N assimilation into biomass (Table 2) have the potential to influence the relative availability of nitrogenous compounds for other metabolic pathways. A common biochemical pathway for assimilation of NH_4^+ into amine groups includes the reaction driven by the glutamine synthetase enzyme (Myrold, 1998). This reaction consumes one ATP, so we assume the energy required for N assimilation via this reaction was the free energy required by the reverse of the hydrolysis reaction that produces one ATP from ADP ($m_{G,NH_4^+} = 31.8$ kJ mol−N−assimilated^{-1}) (Madigan et al., 2003). Assimilation of NO_3^- or NO_2^- requires reduction of the associated N before the resulting NH_4^+ can be incorporated into biomass. This reduction is driven by assimilative nitrate and nitrite reductase enzymes (Myrold, 1998). Biological reduction of compounds commonly requires NADH as an electron source ($2e^-$ per NADH) (Vallino et al., 1996; Madigan et al., 2003). Therefore, we assumed that the energy necessary to assimilate NO_3^- and NO_2^- can be derived from the free energy required by the half reaction that produces NADH from NAD^+ (30.9 kJ per e^-). Following this logic, NO_3^- assimilation requires four NADH plus the one ATP necessary to assimilate the resulting NH_4^+($m_{G,NO_3^-} =$ 155 kJ mol−N−assimilated^{-1}), and NO_2^- assimilation requires three NADH plus one ATP ($m_{G,NO_2^-} = 125$ mol−N−assimilated^{-1}). These estimates are theoretical and may not accurately represent the total energy required for N assimilation. Thus, this approach may be inaccurate when availability of energy limits N assimilation, which is probably not a common scenario for microbial assemblages that do not fix N. However, the relative ranks of these estimated costs of N assimilation will force the optimization to estimate N assimilation into biomass in the appropriate order of energetic efficiency, which NH_4^+($m_{G,NO_3^-} = 155$ kJ mol−N−assimilated^{-1})h is from highest to lowest: NH_4^+, NO_2^-, and NO_3^-.

As implemented in this model, the apparent effect of Monod kinetics as a function of solute concentrations may be influenced by numerous physical and biological mechanisms governing solute dynamics in microbial ecosystems, including physical boundary layer behavior, diffusion rate limitation into and within biofilms, and kinetic rate limitation by biochemical reactions. Thus, comparison of model behavior to laboratory experiments will ultimately require that Monod kinetic parameters are adjustable on a compound-by-compound basis. However, we wished to avoid any confounding influence of variability in Monod kinetics during initial model tests, when our primary goal was to assess the appropriate behavior of thermodynamic controls in the model. Therefore, we chose to set the Monod parameters to the same values for all compounds, where for each compound X: $U_{XB,max} = 0.435$mmol-X mmol-C-biomass^{-1} h^{-1} and $C_{X,half} = 2.83$ mmol-X L^{-1}. These values were based on an average of values for C uptake across multiple types of DOC (Peil and Gaudy, Jr., 1971).

The microbial turnover rate was set to $d_{TO} = 0.019$ h^{-1} (i.e., 1.9% of biomass decays per hour). This value is based on an average of estimates from planktonic aquatic bacteria (Servais et al., 1985). This value is also within the range of estimates from heterotrophic bacteria reported by van Loosdrecht and Henze (1999), and is near the value considered typical for heterotrophic bacteria (0.017 h^{-1}) by Henze et al. (2000).

3.2. Initial conditions and scenarios for model assessment

Default values for initial microbial biomass (0.56 mmol-C), initial DOC concentration (1.3 mmol-C L^{-1}), and water volume (62.2 mL) in simulated batch reactors were based on measurements from laboratory slurry experiments performed on wetland soils (Burgin unpublished). In the current model, the C:N ratio in biomass is maintained at the Redfield ratio (106:16). For testing purposes, we did not wish for heterotrophs to compete for inorganic N in the simulated batch reactors, unless otherwise specified. Therefore, the default initial DON concentration was set such that the available DOC:DON ratio was equal to that of the biomass (i.e., according to the Redfield ratio, or initial DON concentration = 0.196 mmol-N L^{-1}). Default initial concentrations of electron acceptors DO, NO_3^-, and SO_4^{-2} were all set to 0.28 mmol L^{-1}, which is the saturation concentration of DO at standard atmospheric pressure and 20 °C.

Multiple simulation scenarios were executed by varying the default initial conditions, where differences in initial conditions were designed to promote varying levels of competition among microbial functional groups capable of different metabolic pathways. Scenarios focused on 3 areas of competition for the following resources (Table 4): (1) DOC as an energy source and electron donor, (2) DO as a TEA, and (3) N as an electron donor, TEA, and element necessary for growth.

Scenario 1: competition for DOC

DOC is a source of electrons, energy, and carbon for organo-chemo-heterotrophic microbes. The dominant heterotrophic metabolic processes are determined by the outcome of competition for DOC among microbes capable of different oxidizing reactions. Initial conditions for this scenario were configured to promote heterotrophic oxidation of DOC using O_2, NO_3^-, and SO_4^{-2} as TEAs. In addition to the intermediate default DOC concentration (Table 4, simulation 1b), simulations were conducted at lower and higher initial DOC concentrations. The lower concentration was 0.28 mmol-C L^{-1}, equal to the TEA concentrations (Table 4, simulation 1a). The higher concentration was 2.83 mmol-C L^{-1}, equal to the half-saturation concentration used as the Monod kinetic parameter (Table 4, simulation 1c). Initial DON concentrations were adjusted such that initial DOC:DON ratios were always 106:16. Results from these simulations were assessed to ensure that the appropriate order of metabolic reactions occurred through the numerical experiments when competition for energy among heterotrophs was high.

Scenario 2: competition for DO

DO is used as an oxidizing agent by both heterotrophic and autotrophic microbes. For example, the dominant metabolic use of DO in oxic systems is determined by the outcome of competition for DO between nitrifiers and aerobic heterotrophs. Starting with the lower initial DOC concentration in simulation 1a (0.28 mmol-C L^{-1}), initial concentration of NH_4^+ for this scenario was adjusted to two different levels to promote varying levels of competition between nitrifiers and aerobic heterotrophs for DO. For the lower level, initial NH_4^+ concentration was set to 0.07 mmol L^{-1}, equal to one fourth the initial DOC concentration (Table 4, simulation 2a). For the higher level, initial NH_4^+ concentration was set to 0.28 mmol L^{-1}, equal to the initial DOC concentration (Table 4, simulation 2b). All initial inorganic nitrogen was assumed to be in the form of NH_4^+, thus NO_3^- concentrations were set to 0. Results from these simulations were assessed to ensure that the relative abundance of NH_4^+, DOC, and DO appropriately influenced the rates of nitrification and aerobic respiration.

Scenario 3: competition for N

More realistic simulations are likely to include poorer quality DOM,with respect to the amount of DON available for assimilation. In these cases, metabolic use of available N is determined by the outcome of competition among autotrophs and heterotrophs for inorganic N assimilation, when heterotrophic N demand is not satisfied by DON alone. Again starting with the lower initial DOC

Table 4
List of initial conditions used for testing scenarios.

Variable	Value	Unit	Description
Default			
$B_{t=0}$	0.56	mmol-C	Default initial biomass concentration
C_{DOC}	1.3	mmol-C L^{-1}	Default initial dissolved organic carbon concentration
C_{DON}	0.196	mmol-N L^{-1}	Default initial dissolved organic nitrogen concentration (according to Redfield ratio)
C_{DO}	0.28	mmol-O_2 L^{-1}	Default initial dissolved oxygen concentration
$C_{NO_3^-}$	0.28	mmol-N L^{-1}	Default initial nitrate concentration
$C_{SO_4^{-2}}$	0.28	mmol-S L^{-1}	Default initial sulfate concentration
$C_{NH_4^+}$	0	mmol-N L^{-1}	Default initial ammonium concentration
C_{CH_4}	0	mmol-C L^{-1}	Default initial methane concentration
Scenario 1			Competition for DOC
Simulation 1a			Lower DOC level
C_{DOC}	0.28	mmol-C L^{-1}	Set to the same concentration as default TEA concentrations
C_{DON}	0.0423	mmol-N L^{-1}	According to Redfield ratio
Simulation 1b			Default (intermediate) DOC level
–			Applied defaults
Simulation 1c			Higher DOC level
C_{DOC}	2.83	mmol-C L^{-1}	Set to the half-saturation concentration (Monod parameter)
C_{DON}	0.427	mmol-N L^{-1}	According to Redfield ratio
Scenario 2			Competition for DO
Simulation 2a			Lower NH_4^+ level
C_{DOC}	0.28	mmol-C L^{-1}	Lower DOC level from scenario 1
$C_{NH_4^+}$	0.07	mmol-N L^{-1}	One fourth the DOC and DO concentration
$C_{NO_3^-}$	0	mmol-N L^{-1}	Assuming all inorganic N in the form of NH_4^+
Simulation 2b			Higher NH_4^+ level
C_{DOC}	0.28	mmol-C L^{-1}	Lower DOC level from scenario 1
$C_{NH_4^+}$	0.28	mmol-N L^{-1}	Equal to DOC and DO concentration
$C_{NO_3^-}$	0	mmol-N L^{-1}	Assuming all inorganic N in the form of NH_4^+
Scenario 3			Competition for N
Simulation 3a			Lower DON level
C_{DOC}	0.28	mmol-C L^{-1}	Lower DOC level from scenario 1
C_{DON}	0.0106	mmol-N L^{-1}	According to 4 times the Redfield ratio
Simulation 3b			Lower DON level with NH_4^+
C_{DOC}	0.28	mmol-C L^{-1}	Lower DOC level from scenario 1
C_{DON}	0.0106	mmol-N L^{-1}	According to 4 times the Redfield ratio
$C_{NH_4^+}$	0.01	mmol-N L^{-1}	Added for inorganic N supply in NH_4^+ form

concentration in simulation 1a, the initial DON concentrations for this scenario were varied in order to force heterotrophs to assimilate inorganic forms of N for growth. Initial DON concentrations were lowered to 0.0106 mmol-N L^{-1}, such that the initial DOC:DON ratio was increased to 106:4 (Table 4, simulation 3a). Results from this simulation were assessed to ensure the appropriate outcome of competition between heterotrophs and autotrophs for inorganic N. Furthermore, an additional simulation was executed with a small amount of initial NH_4^+ (Table 4, simulation 3b). Results of this simulation were assessed to ensure that the more energetically inexpensive form of inorganic nitrogen assimilation was preferred.

4. Model test results and interpretation

We selected specific illustrations from the full output from the simulation environment (e.g., Fig. 3) to demonstrate pertinent patterns in model behavior used to assess the three testing scenarios. We interpret model test results as indicative of effective simulated competition between functional groups of microbes (in the sense of van de Leemput et al., 2011). More detailed model output for all testing scenarios is available in the Supplemental materials (Figs. S1–S7).

4.1. Scenario 1: competition for DOC

Simulations from scenario 1 demonstrated that the initial DOC concentration influenced the degree to which different types of metabolic reaction could occur simultaneously (Fig. 4). During the simulation with lower initial DOC concentrations (simulation 1a, Fig. 4a), a single type of metabolic reaction tended to dominate until the TEA necessary for that reaction was depleted. The order of dominant metabolic pathways progressed from higher energy yielding reactions (e.g., aerobic respiration from ca. 0 to 1 h) to lower energy yielding reactions (e.g., sulfate reduction from ca. 4.5 to 5 h). Lower initial DOC concentrations thus produced a simulation of higher competition among heterotrophs, where the microbes capable of higher energy-yielding reactions outcompeted those capable of lower energy-yielding reactions.

In simulations starting with incrementally higher DOC concentrations (simulation 1b and c), different metabolic pathways were more likely to occur simultaneously. During the simulation with intermediate initial DOC concentration (simulation 1b, Fig. 4b), aerobic respiration of DOC and denitrification occurred simultaneously between 0 and 2 h. During the simulation with higher DOC concentration (simulation 1c, Fig. 4c), simulated aerobic respiration of DOC, denitrification, and sulfate reduction occurred simultaneously between 0 and 2 h. Increased co-occurrence of metabolic pathways with increased DOC availability indicates a decrease in the simulated competition for DOC among heterotrophs, as resources other than DOC became limiting.

At lower and intermediate DOC concentrations (simulation 1a and b, Fig. 4a and b), modest rates of nitrification were made possible by DO availability and NH_4^+ generation by mineralization of organic matter. Lower initial DOC concentration and competition for DOC among heterotrophs thus provided a modest competitive advantage for autotrophic nitrifiers, as indicated by

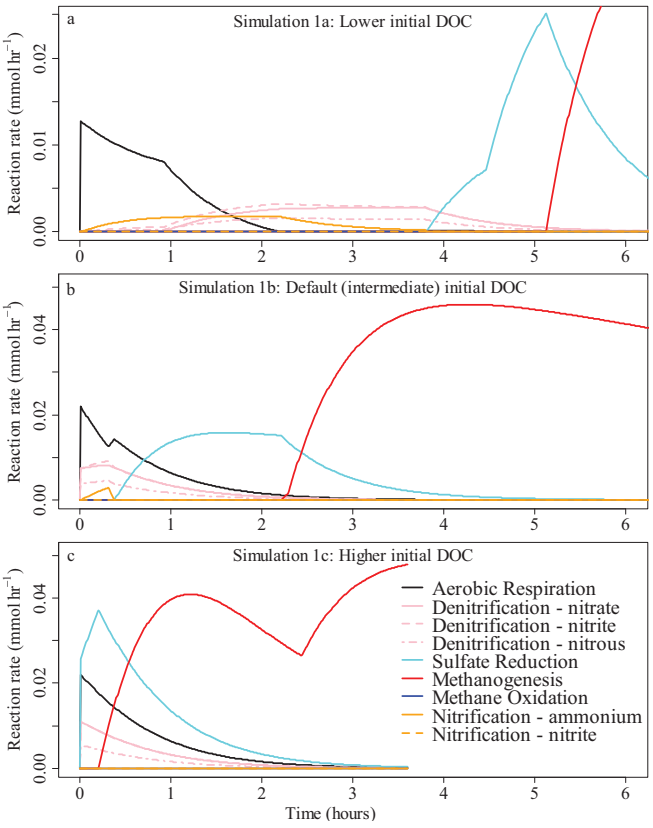

Fig. 4. Metabolic reaction rates from simulations of scenario 1 (competition for DOC), in order of the initial DOC concentration (a) lower initial DOC (simulation 1a), (b) default or intermediate initial DOC (simulation 1b), and (c) higher initial DOC (simulation 1c).

nitrification occurring simultaneously with aerobic respiration during the first 2 h of simulation 1a (Fig. 4a). When initial DOC concentrations were higher and there was minimal competition for DOC among heterotrophs (simulation 1c), nitrification did not occur (Fig. 4c) because DO was more efficiently used by aerobic heterotrophs.

4.2. Scenario 2: competition for DO

Higher initial NH_4^+ concentrations in scenario 2 resulted in higher rates of nitrification relative to aerobic respiration of DOC in simulated batch reactors (Fig. 5). During the simulation with lower initial NH_4^+ concentration (simulation 2a, Fig. 5a), nitrification and aerobic respiration of DOC occurred simultaneously. As described in Section 4.1, the ability of nitrifiers to compete for DO is at least in part supported by limited availability of DOC for aerobic respiration. Nitrification thus inhibited aerobic respiration of DOC to some degree, until around hour 0.8 when resources were depleted to the point that exclusive aerobic respiration of DOC was the more energetically efficient use of DO. A similar, but exaggerated, pattern occurred during the simulation with a higher initial NH_4^+ concentration (simulation 2b, Figs. 3 and 5b), to the degree that nitrification dominated aerobic respiration of DOC for a short period of time. Taken together, these results show how the outcome of competition for DO between autotrophs and heterotrophs is determined by a complex interaction of the availabilities of DO, DOC, and NH_4^+, but this complexity can be summarized and predicted systematically by energetic constraints in the optimization scheme.

In both simulation 2a and b, nitrification of NH_4^+ produces NO_2^- early in the simulation, which stimulates heterotrophic denitrification of the available NO_2^-. In these cases, autotrophic nitrification of NO_2^- does not occur because when DOC is available, the overall energetic yield of heterotrophic denitrification of NO_2^- and N_2O are quite high relative to the energetic yield of autotrophic nitrification of NO_2^- (Table 1). This would suggest heterotrophs are able to outcompete autotrophs for NO_2^-, even while NH_4^+ nitrifying autotrophs are outcompeting aerobic heterotrophs for DO. Interestingly, the total energy yield of denitrifying NO_2^- to N_2O to N_2 (492 kJ per 0.5 mol acetate, balanced for N) is higher than that of aerobic respiration (437 kJ per 0.5 mol acetate, see total E_S per DOC-C for these reactions in Table 1), such that the competition for DOC by NO_2^- denitrifiers likely results in an additional competitive advantage for NH_4^+ nitrifiers over aerobic heterotrophs for DO. This model result suggests that future studies should consider the energy yields of the incremental reactions of nitrification and denitrification when assessing the outcome of competition between autotrophs and heterotrophs.

4.3. Scenario 3: competition for N

Increasing the initial aqueous DOC:DON ratio by a factor of four resulted in competition for metabolism of inorganic N that did not occur in scenarios 1 or 2. Assimilation of NH_4^+ by aerobic heterotrophs apparently inhibited the nitrification that was observed during the first hour of simulations without initial NH_4^+ in scenario 1 (Fig. 4a vs. Fig. 6c) and with initial NH_4^+ in scenario 2 (Fig. 5a vs. Fig. 6c). Nitrification did not occur in either simulation 3a or b until demand for NH_4^+ and DO by aerobic heterotrophs waned. In this situation, the model effectively predicts that aerobic heterotrophs can outcompete nitrifiers for NH_4^+, likely due to the lower energy requirements of heterotrophic growth relative to autotrophic growth.

When there was no initial NH_4^+ (simulation 3a), NO_3^- assimilation dominated until NH_4^+ was made available by mineralization (Fig. 6b). When NH_4^+ was made available initially

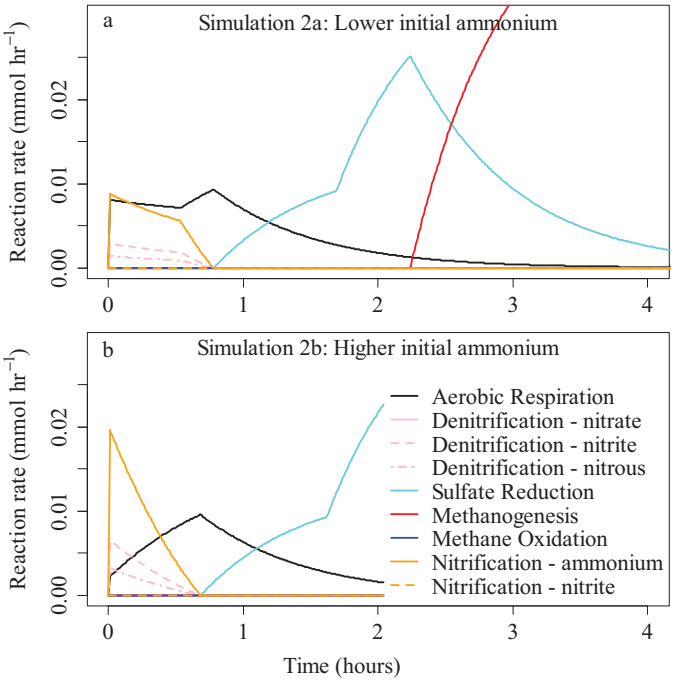

Fig. 5. Metabolic reaction rates from simulations of scenario 2 (competition for DO), in order of initial NH_4^+ concentration (a) lower initial NH_4^+ concentration (simulation 2a) and (b) higher initial NH_4^+ concentration (simulation 2b).

(simulation 3b), NH_4^+ assimilation was preferred over NO_3^- assimilation (Fig. 6d).

5. Discussion

Model results demonstrate how thermodynamic principles help quantify the energetic mechanisms of functional competition among various microbial metabolic groups. Simulated competition for a given energy source was indicated by the degree to which different types of heterotrophic metabolic reactions occurred simultaneously in scenario 1. Higher competition for DOC resulted in little simultaneous occurrence of different types of reactions (Fig. 4a), and decreasing competition for DOC resulted in increasing co-occurrence of different types of reactions (Fig. 4b and c). Simulated competition for a TEA (in this case DO) was indicated by the relative levels of nitrification and aerobic respiration with changes in NH_4^+ availability in scenario 2. Nitrifiers were more competitive with aerobic heterotrophs for DO when NH_4^+ availability was high relative to DOC (Fig. 5b). Finally, simulated competition for N as both an energy source and nutrient was evident when heterotrophs required inorganic N for growth in scenario 3. Aerobic heterotrophs tended to outcompete nitrifiers for inorganic N, and microbes in general used the most energy-efficient form of inorganic N assimilation available (Fig. 6a–d). Taken together, these three testing scenarios demonstrate how the general thermodynamic and stoichiometric constraints on anabolic and catabolic metabolism can be addressed concurrently and succinctly in a single model. This approach results in a biogeochemical modeling framework capable of simulating complex patterns of functional competition for energy and compounds in a wide range of aqueous environments.

Because the model utilizes optimization of multiple linear constraints, all of these elements of competition can be accounted for simultaneously during each simulation time step. Evidence for the influence of overlapping competitive relationships was demonstrated by the simulated competitive advantage for DO provided to nitrifiers by the simultaneous competition for DOC among heterotrophs (scenario 1). Furthermore, the design of the generalized optimization scheme and the highly modular NEO model allow for relatively straightforward extension to account for other forms of competition for compounds, such as further competition for DOC by heterotrophic ferric iron reducers, further competition for DO by autotrophic sulfide oxidizers, and further competition for nutrients based on phosphorus demand. This type of flexibility in model implementation will enable an adaptive hypothesis testing cycle for the study of complex biogeochemical systems.

5.1. A benchmark in parsimony for adaptive hypothesis testing

We suggest that this model represents a benchmark of maximum parsimony relative to community structure, DOC quality, energy yield, and competition. Comparison of new variants of this model with this established benchmark will be a critical step toward maintaining maximum parsimony when assessing the need for more complex model structure. For example, we found in initial model tests that microbial assemblage structure had to be functionally categorized by the form of carbon assimilated, hence our adaptation to a carbon source specific model that tracks activity of autotrophs, heterotrophs, and methanotrophs separately. Without this separation, the simulated combinations of metabolic pathways were frequently unrealistic because growth could come from incompatible sources of energy and carbon. For example, the total simulated biomass might increase with organic carbon as a sole source for growth (heterotrophic process) at the same time as nitrification was the sole source for energy (autotrophic process). Therefore, we found that the carbon source specific model embodied a critical element of structural complexity necessary to ensure that the form of carbon assimilated for growth was compatible with the energy source used to fuel that growth. The carbon source specific model is still abstract relative to the oxidizing agent used. For example, the standing stock of heterotrophs are considered in bulk and can thus can instantaneously switch between uses of different TEAs. Therefore, the current model may provide unrealistic simulations when the available compounds are changing rapidly, and may underestimate the time it takes the microbial assemblage to switch between different metabolic processes. The modularity of the model allows biomass to be separated into more compartments (e.g., “reaction specific”, “species specific”, or “gene specific” models), should this become an element of complexity necessary to describe observed biogeochemical patterns. However, we would hesitate to add this complexity unless a given data set provided significant evidence that it was necessary, just as we hesitated to break up the total microbial biomass into carbon source specific functional groups until it was proven necessary.

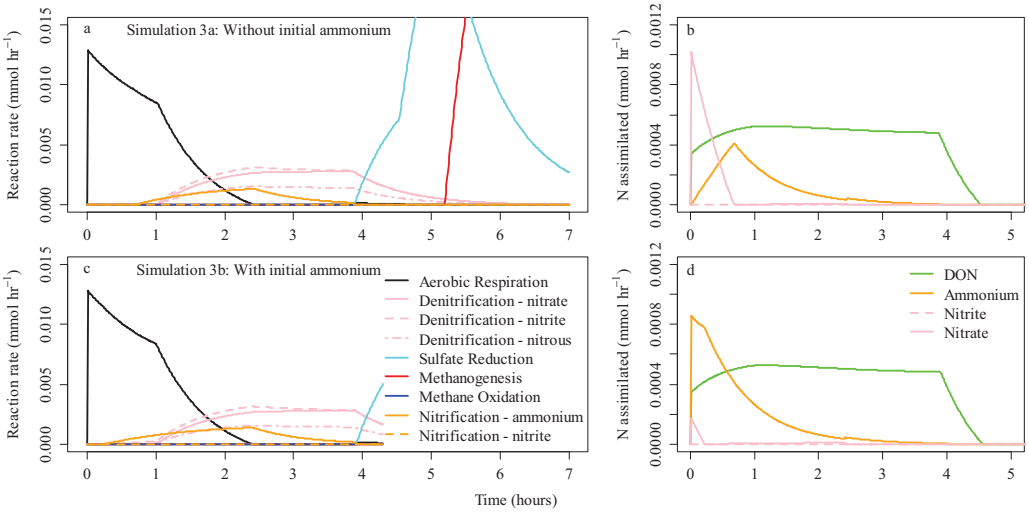

Fig. 6. (a and c) Metabolic reaction rates and (b and d) N assimilation rates from simulations of scenario 3 (competition for N), including (a and b) simulation without initial NH_4^+ concentration (simulation 3a) and (c and d) simulation with initial NH_4^+ concentration (simulation 3b).

The model also represents a benchmark in parsimony by assuming uniform quality of DOC. We recognize that additional complexity in tracking DOC quality will likely be necessary in comparisons with observations of real systems, particularly with respect to the role of fermentation of refractory DOC into labile DOC in anoxic systems. To add this complexity, DOC compounds of varying quality could be tracked as different compounds or categories of compounds in the model (e.g., Vallino et al., 1996), similar to the separation of generic DOC and CH_4 in the current model.

For this effort, we have established the standard free energy of reaction as a simple benchmark for calculation of metabolic energy yield (e.g., Table 1). Not all simulated systems are likely to reflect yields assumed from standard conditions, and thus the standard free energy of reaction may be a poor reflection of the true energy yield of a given reaction. For more extreme chemical conditions (e.g., very low pH), the model may be adapted to recalculate E_S from the equilibrium constant of each reaction based on some sort of effective compound concentration in the biologically available node, should the use of standard free energy prove to be a significant source of error in model predictions. Derivation of algorithms that could reasonably estimate these effective concentrations would not be trivial and would involve a far more detailed simulation of biofilm behavior than is incorporated in the current model.

Finally, this model represents a benchmark in parsimony for the fundamental mechanisms behind microbial competition. We acknowledge the model does not represent the full spectrum of competitive mechanisms necessary to predict the diversity of competitive outcomes observable in nature. Rather, the tests of the model should be interpreted as a principled assessment of the competitive behaviors that may emerge from fundamental kinetic, stoichiometric, and thermodynamic theory. For example, simultaneous occurrence of aerobic respiration, denitrification, and sulfate reduction in an oxic environment may not be as common as this model would predict when DOC is not limiting (Fig. 4c). This model behavior occurs because the only mechanism of competition considered in this scenario is thermodynamic in nature (i.e., over the energy in DOC), and for testing purposes we are assuming that all kinetic uptake parameters are equal. Many other mechanisms of competition not currently implemented in the model are likely to explain how aerobic microbes outcompete anaerobes in an oxic environment. For example, competition over space or the excretion of inhibitory compounds may be important to the outcomes of microbial competition in a real system. Likewise, other forms of competition or inhibition will likely come into play before there is direct competition between nitrifiers and aerobic heterotrophs over DO. That being said, the model is designed to be highly extensible, allowing other forms of competition to be implemented, either through a more complex calculation of the rate-limiting uptake of compounds in the NEO model, or through more complex calculation of parameters for the optimization scheme. Our approach provides a path for scientific workflow where features representing more complex forms of competition can be relatively easily implemented and compared to the current fundamental benchmark.

5.2. Comparison with previous models

The novelty of the presented model does not derive from of a new way of thinking about any given control on microbial metabolism. Its novelty does derive from a new way of incorporating multiple existing ideas about controls on metabolism into a more generalized, modular, and extensible software architecture, which facilitates assessment of additional simulated metabolic complexity with minimal additional code development. All characteristics of the optimization scheme and governing model structure come nearly directly from published models or well-established thermochemical theory. The biologically available node and biomass node of the NEO model structure are similar to the metabolite pool and biomass compartments suggested by Franklin et al. (2011). Within this structure, we incorporated a simulation sequence of solute dynamics similar to the model put forth by Menkel and Knights (1995), which included uptake via Monod kinetic equations, processing by metabolic activity, and calculation of microbial growth. The application of thermodynamic and stoichiometric constraints in an optimization scheme to maximize biomass was suggested by Vallino et al., (1996) and was also utilized by Boyle and Morgan (2011). Van de Leemput et al. (2011) also used a more explicit formulation of thermodynamic and stoichiometric equations to predict metabolic pathways of N. Vallino (2010) further generalized the thermodynamic approach based on maximized entropy production.

Not surprisingly, the behavior of the presented model is comparable to that of previous models based on similar principles, even when those models used a different approach to conceptual or mathematical implementation. Hedin et al. (1998) defined a statistical approach for predicting the order of TEA utilization, and tested their model against patterns observed in groundwater ecosystems near streams. The model we present predicts the same pattern (scenario 1), but is based on a more mechanistic implementation that simulates TEA utilization rates as a function of both relative energy yields and kinetic rate-limitation. The work of van de Leemput et al. (2011) shows how commonly observed nitrogen dynamics can be predicted from a relatively concise set of thermodynamic constraints, even when no prior knowledge of observed N pathways is assumed. The presented model has not yet been configured to replicate their exhaustive tests of the balance between potential N metabolic pathways. But it could be, and it currently does predict similar behavior in terms of the balance between aerobic respiration of DOC and nitrification under oxic conditions (scenario 2). Vallino et al. (1996) presented a similar optimization scheme for addressing the role of carbon quality in bacterial metabolism and growth. The presented model shows similar behavior in terms of heterotrophic use of inorganic N when available DOM has low DON content, and also shows the assimilative preference for the more reduced forms of inorganic N (scenario 3). We are encouraged by these similarities, in that they suggest the presented model captures the fundamental principles of these models in a single generalized thermodynamic formulation, in addition to the ability to simulate rate-limitation.

5.3. Model extensibility and future applications

The current work has focused on development of the theory and implementation of our approach to simulation of generalized microbial ecosystem behavior and the resulting biogeochemical dynamics. However, our intention in the near future is to use this model to test hypotheses about spatial and temporal patterns observed in field and lab data from a restored wetland (Ardón et al., 2013). In its current form, this model is not likely to be an adequate descriptor of many of the complexities found in real microbial ecosystems. The usefulness of the model derives from our ability to faithfully simulate how widely accepted concepts of thermodynamics, stoichiometry, and kinetics may be used to quantify rates of metabolic processes. Then, we can assess the residual error between model predictions and field or laboratory observations to generate new hypotheses about the behavior of our study system. These new hypotheses may correspond to errors in the original assumptions about the current model constraints, or the addition

of new model constraints that are not related to thermodynamic or stoichiometric theory (see examples in Section 5.1).

To support testing of new hypotheses, the model was designed to be extensible in two primary directions: (1) addition of new biogeochemical constraints and (2) integration with hydrologic models. Use of the NEO framework facilitates both of these goals. Constraints are added to the optimization scheme simply by adding equations to the linear program (see Appendix A). To track the effects of that new constraint, additional compounds can be added to the NEO packages that govern the time series model (Fig. 1), without the need to change any of the existing code. Additional code abstraction and automation of linear program code generation will further facilitate extensibility of metabolic features. Finally, any additional configuration information required by the new metabolic behavior can be relatively easily added to the batch reactor simulation environment. Integration of the NEO microbial ecosystem model with a NEO hydrologic model will be achieved via two mechanisms: (1) model overlap within the shared state space of aqueous nodes and (2) addition of advection and diffusion behaviors to the solute models.

More generally, we envision this model, and others like it, as a useful tool for addressing the uncertainty of predicting biogeochemical trajectories in a changing world. The complex interactions of land use change and climate change are introducing unprecedented mixtures of electron donors and acceptors to microbial ecosystems. For example, our study wetland is simultaneously experiencing reestablishment of saturated conditions in formerly agricultural soils along with brackish water incursion via surface water that will presumably increase with sea level rise (Ardón et al., 2013). This creates potential for complexity in biogeochemical interactions and nutrient limitation that require a mechanistic model and computer assistance to analyze, especially considering the lack of history of similar conditions. The number of ecosystems experiencing dramatic changes in external forcing will presumably increase in the coming decades, and we suggest comparisons of alternative mechanistic models will prove to be a valuable tool in understanding their potential resulting trajectories.

6. Summary and conclusions

We have demonstrated an extensible modeling system for simulating simultaneous thermodynamic competition for energy, terminal electron acceptors, and nutrients in microbial ecosystems. The model is based on an aggregation of established thermodynamic, stoichiometric, and kinetic ecological theories. Model tests were conducted based on hypothetical scenarios imposed on a closed-system batch reactor simulation environment. Model tests have shown that the model can predict the thermodynamically appropriate order of dominance of various metabolic processes in closed-system batch reactor simulations. Model tests have also demonstrated the potential for complex interactive effects when considering all limiting factors in competitive relationships together. We suggest that the NEO-based model framework is sufficiently general and extensible to be applied to a broad range of biogeochemical analyses in microbial ecosystems. We also suggest that the current form of the model represents a useful benchmark in maximized parsimony, allowing an informative assessment of the residual errors in comparisons of model predictions to field and laboratory observations. Exploration of these residuals will ultimately provide us with a structured, objective, and principled approach to assessing new hypotheses about the nature of microbial competition, and the ability of the microbial ecosystem to determine the biogeochemical trajectory of our study system.

Acknowledgements

Thank you to Marcelo Ardón and the research team at the Timberlake Observatory for Wetland Restoration for their support and feedback on ideas. Thank you to Isaac Griffith, Ryan Nix and the NEO development team for their support on the modeling framework. We thank Brian Fath, Maury Valett, and two anonymous reviewers for their thoughtful comments. This material is based on work supported by the National Science Foundation grant # DEB-1021001 and from the Montana Institute on Ecosystems' award from the National Science Foundation EPSCoR Track-1 program under grant # EPS-1101342.

Appendix A. : code for the linear optimization

The following code is written for lp_solve (v. 5.5.2.0, http://lpsolve.sourceforge.net), and is used to perform the optimization of metabolic processes for each time step in the NEO model. Optimization is based on finding a unique solution to a series of linear constraints that will maximize the biomass remaining at the end of each time step. Design of constraints was based on mass balance, energy balance, andfinding the most energetically efficient use of the available chemical compounds (see Section 2.2).

```
/*
   OBJECTIVE FUNCTION: Maximize the remaining biomass
*/

max: BiomassRemaining;

/*
   RESOURCE AVAILABILITIES: Place-holders where values are
   replaced by the NEO model
*/

/* Biomass */

HetBiomass = 0.0;      /* Heterotrophic biomass */
AutoBiomass = 0.0;     /* Autotrophic biomass */
MethBiomass = 0.0;     /* Methanotrophic biomass */

/* Availability of dissolved aqueous chemical species */
```

```
    DOCAvail = 0.0;        /* Dissolved organic carbon */
    DONAvail = 0.0;        /* Dissolved organic nitrogen */
    DiOxygenAvail = 0.0;   /* Dioxygen */
    NitrateAvail = 0.0;    /* Nitrate */
    N2OAvail = 0.0;        /* Nitrous oxide */
    NitriteAvail = 0.0;    /* Nitrite */
    AmmoniumAvail = 0.0;   /* Ammonium */
    MethaneAvail = 0.0;    /* Methane */
    SulfateAvail = 0.0;    /* Sulfate */

    /*
       TOTAL BIOMASS: Microbial biomass separated by carbon source
    */

    BiomassRemaining >= 0;
    HetBiomassRemaining >= 0;
    AutoBiomassRemaining >= 0;
    MethBiomassRemaining >= 0;

    BiomassRemaining = HetBiomassRemaining + AutoBiomassRemaining
                     + MethBiomassRemaining;

    TotalGrowth >= 0;
    HetGrowth >= 0;
    AutoGrowth >= 0;
    MethGrowth >= 0;
    TotalGrowth = HetGrowth + AutoGrowth + MethGrowth;

/*
   OPTIMIZATION CONTSTRAINTS ON GROWTH FOR EACH METABOLIC GROUP
*/

/*
   HETEROTROPHS
*/

/* Heterotrophic pathways */

/* Aerobic respiration */
/* DOC + O2 --> CO2 */

AerobicResp >= 0;

/* Methanogenesis from using DOC as a TEA */
/* DOC --> CH4 */

Methanogenesis >= 0;

/* Denitrification of nitrate */
/* DOC + NO3 --> NO2 */

DenitNitrateRed >= 0;

/* Denitrification of nitrite */
/* DOC + NO2 --> N2O */

DenitNitriteRedN2O >= 0;

/* Denitrification of nitrous oxide */
/* DOC + N2O --> N2 */

DenitN2ORedN2 >= 0;

/* Sulrate reduction */
/* DOC + SO4 --> HS */

SulfateRed >= 0;
```

```
 /* Energy demand of heterotrophs */

 HetMaintEnergyRequired >= 0;
 /* Added by NEO: HetMaintEnergyRequired =
                      x HetBiomass + x HetBiomassRemaining; */

 HetGrowthEnergyRequired >= 0;
 DOCAssimilated >= 0;
 HetAmmoniumAssimilated >= 0;
 HetNitrateAssimilated >= 0;
 HetNitriteAssimilated >= 0;
 /* Numbers in kJ/umol */
 HetGrowthEnergyRequired = 4.32E-04 DOCAssimilated + 3.18E-05 HetAmmoniumAssimilated
                         + 1.25E-04 HetNitriteAssimilated + 1.55E-04
 HetNitrateAssimilated;
 HetEnergyRequired >= 0;
 HetEnergyRequired = HetMaintEnergyRequired + HetGrowthEnergyRequired;

/* Heterotrophic growth constraints */
HetGrowth >= 0;
HetNAssimilated >= 0;
HetNAssimilated = 0.1509 HetGrowth;
HetDONAssimilated >= 0;
HetNAssimilated = HetAmmoniumAssimilated + HetNitrateAssimilated
                + HetNitriteAssimilated + HetDONAssimilated;

/* Energy supplied by heterotrophic reactions */
HetEnergySupplied >= 0;
/* Numbers in kJ/umol */
HetEnergySupplied = 4.37E-04 AerobicResp + 2.88E-04 DenitNitrateRed
                  + 4.15E-04 DenitNitriteRedN2O + 6.45E-04 DenitN2ORedN2
                  + 3.8E-05 SulfateRed + 2.8E-05 Methanogenesis;

/* Balance energy and carbon for heterotrophs. */
HetEnergySupplied = HetEnergyRequired;
HetBiomassDeath >= 0;
HetBiomassRemaining = HetBiomass + HetGrowth - HetBiomassDeath;

/*
   AUTOTROPHS
*/

/* Autotrophic pathways */

/* Nitrification of ammonium */
/* NH4 + O2 --> NO2 */

NitrAmmOxid >= 0;

/* Nitrification of nitrite */
/* NO2 + O2 --> NO3 */

NitrNitOxid >= 0;

/* Energy demand of autotrophs */

AutoMaintEnergyRequired >= 0;
/* Added by NEO: AutoMaintEnergyRequired =
                   x AutoBiomass + x AutoBiomassRemaining; */

AutoGrowthEnergyRequired >= 0;
CO2Assimilated >= 0;
AutoAmmoniumAssimilated >= 0;
AutoNitrateAssimilated >= 0;
AutoNitriteAssimilated >= 0;
/* Numbers in kJ/umol */
AutoGrowthEnergyRequired = 3.5E-03 CO2Assimilated + 3.18E-05 AutoAmmoniumAssimilated
                         + 1.25E-04 AutoNitriteAssimilated + 1.55E-04
```

```
 AutoNitrateAssimilated;
 AutoEnergyRequired >= 0;
 AutoEnergyRequired = AutoMaintEnergyRequired + AutoGrowthEnergyRequired;

 /* Autotrophic growth constraints */
 AutoNAssimilated >= 0;
 AutoNAssimilated = 0.1509 AutoGrowth;
 AutoNAssimilated = AutoAmmoniumAssimilated + AutoNitrateAssimilated
                  + AutoNitriteAssimilated;

/* Energy supplied by autotrophic reactions */
AutoEnergySupplied >= 0;
/* Numbers in kJ/umol */
AutoEnergySupplied = 1.83E-04 NitrAmmOxid + 1.48E-04 NitrNitOxid;

/* Balance energy and carbon for autotrophs */
AutoEnergySupplied = AutoEnergyRequired;
AutoBiomassDeath >= 0;
AutoBiomassRemaining = AutoBiomass + AutoGrowth - AutoBiomassDeath;

/*
   METHANOTROPHS
*/

/* Methanotrophic pathways */

/* Methanotrophy (complete) */
/* CH4 + O2 --> CO2 */

MethaneOxid >= 0;

/* Energy demand of methanotrophs */

MethMaintEnergyRequired >= 0;
/* Added by NEO: MethMaintEnergyRequired =
                  x MethBiomass + x MethBiomassRemaining; */

MethGrowthEnergyRequired >= 0;
MethAssimilated >= 0;
MethAmmoniumAssimilated >= 0;
MethNitrateAssimilated >= 0;
MethNitriteAssimilated >= 0;
/* Numbers in kJ/umol */
MethGrowthEnergyRequired = 1.09E-03 MethAssimilated + 3.18E-05 MethAmmoniumAssimilated
                         + 1.25E-04 MethNitriteAssimilated + 1.55E-04
MethNitrateAssimilated;
MethEnergyRequired >= 0;
MethEnergyRequired = MethMaintEnergyRequired + MethGrowthEnergyRequired;

/* Methanotrophic growth constraints */
MethGrowth >= 0;
MethNAssimilated >= 0;
MethNAssimilated = 0.1509 MethGrowth;
MethNAssimilated = MethAmmoniumAssimilated + MethNitrateAssimilated
                 + MethNitriteAssimilated;

/* Energy supplied by methanotrophic reactions */
MethEnergySupplied >= 0;
/* Numbers in kJ/umol */
MethEnergySupplied = 4.09E-04 MethaneOxid;

/* Balance energy and carbon for methanotrophs */
MethEnergySupplied = MethEnergyRequired;
MethBiomassDeath >= 0;
MethBiomassRemaining = MethBiomass + MethGrowth - MethBiomassDeath;
```

```
/*
   STOICHIOMETRIC CONSTRAINTS
*/

/* Constrain DOC use */
DOCRemaining >= 0;
DOCOxidized + HetBiomassDeath = AerobicResp + Methanogenesis + SulfateRed +
            DenitNitrateRed + DenitNitriteRedN2O + DenitN2ORedN2;
DOCAssimilated = HetGrowth;
DOCRemaining = DOCAvail - DOCOxidized - DOCAssimilated;

/* Constrain DON use */
DONRemaining >= 0;
DONAssimilated = HetDONAssimilated;
/* Added by NEO: DONMineralized =
                  <DON:DOC in biologically available pool> DOCOxidized */
DONRemaining = DONAvail - DONMineralized - DONAssimilated;

/* Constrain carbon dioxide use */
CO2Assimilated = AutoGrowth;

/* Constrain ammonium use */
AmmoniumRemaining >= 0;
AmmoniumNitrified >= 0;
AmmoniumNitrified = 0.667 NitrAmmOxid;
AmmoniumAssimilated >= 0;
AmmoniumAssimilated = HetAmmoniumAssimilated + AutoAmmoniumAssimilated
                    + MethAmmoniumAssimilated;
AmmoniumRemaining = AmmoniumAvail - AmmoniumNitrified - AmmoniumAssimilated;

/* Constrain nitrate use */
NitrateRemaining >= 0;
NitrateDenitrified >= 0;
NitrateDenitrified = 2.0 DenitNitrateRed;
NitrateAssimilated >= 0;
NitrateAssimilated = HetNitrateAssimilated + AutoNitrateAssimilated
                   + MethNitrateAssimilated;
NitrateRemaining = NitrateAvail - NitrateDenitrified - NitrateAssimilated;

/* Constrain nitrite use */
NitriteRemaining >= 0;
NitriteOxidized >= 0;
NitriteOxidized = 2.0 NitrNitOxid;
NitriteAssimilated >= 0;
NitriteAssimilated = HetNitriteAssimilated + AutoNitriteAssimilated
                   + MethNitriteAssimilated;
NitriteRemaining = NitriteAvail + 2.0 DenitNitrateRed + AmmoniumNitrified -
            2.0 DenitNitriteRedN2O - NitriteOxidized - NitriteAssimilated;

/* Constrain N2O use */
N2ORemaining >= 0;
N2ORemaining = N2OAvail + 1.0 DenitNitriteRedN2O - 2.0 DenitN2ORedN2;

/* Constrain methane use */
MethaneRemaining >= 0;
MethOxidized >= 0;
MethOxidized = 0.5 MethaneOxid;
MethAssimilated = MethGrowth;
MethGenerated >= 0;
MethGenerated = 0.5 Methanogenesis;
MethOxidized + MethAssimilated <= MethaneAvail;
MethaneRemaining = MethaneAvail + MethGenerated
                 - MethOxidized - MethAssimilated;
```

```
/* Constrain oxygen use */
DiOxygenRemaining >= 0;
DiOxygenUsed >= 0;
DiOxygenUsed = AerobicResp + MethaneOxid + NitrAmmOxid + NitrNitOxid;
DiOxygenRemaining = DiOxygenAvail - DiOxygenUsed;

/* Constrain sulfate use */
/* Sulfate is a TEA for anaerobic heterotrophs */
SulfateRemaining >= 0;
SulfateReduced = 0.5 SulfateRed;
SulfateRemaining = SulfateAvail - SulfateReduced;

/* Calculate CO2 production */
CO2Produced = AerobicResp + DenitNitrateRed + DenitNitriteRedN2O + DenitN2ORedN2
            + SulfateRed + 0.5 MethaneOxid + 0.5 Methanogenesis - CO2Assimilated;
```

Appendix B. Supplementary data

Supplementary data associated with this article can be found, in the online version, at http://dx.doi.org/10.1016/j.ecolmodel.2014.09.003.

References

Allan, J.D., 2004. Landscapes and riverscapes: the influence of land use on stream ecosystems. Annu. Rev. Ecol. Evol. Syst. 35, 257–284.

Ardón, M., Morse, J.L., Colman, B.P., Bernhardt, E.S., 2013. Drought-induced saltwater incursion leads to increased wetland nitrogen export. Global Change Biol. 19 (10), 2976–2985. doi:http://dx.doi.org/10.1111/gcb.12287.

Boyle, N.R., Morgan, J.A., 2011. Computation of metabolic fluxes and efficiencies for biological carbon dioxide fixation. Metab. Eng. 13 (2), 150–158.

Cherif, M., Loreau, M., 2007. Stoichiometric constraints on resource use, competitive interactions, and elemental cycling in microbial decomposers. Am. Nat. 169 (6), 709–724.

Dodds, W.K., et al., 2002. N uptake as a function of concentration in streams. J. N. Am. Benthol. Soc. 21 (2), 206–220. doi:http://dx.doi.org/10.1043/0887-3593(2002)021<0206:N UAAFO>2.0.CO;2.

Fath, B.D., Patten, B.C., Choi, J., 2001. Complementarity of ecological goal functions. J. Theor. Biol. 208 (4), 493–506. doi:http://dx.doi.org/10.1006/jtbi.2000.2234.

Flynn, K.J., 2001. A mechanistic model for describing dynamic multi-nutrient light, temperature interactions in phytoplankton. J. Plankton Res. 23 (9), 977–997.

Franklin, O., Hall, E.K., Kaiser, C., Battin, T.J., Richter, A., 2011. Optimization of biomass composition explains microbial growth-stoichiometry relationships. Am. Nat. 177 (2), E29–E42. doi:http://dx.doi.org/10.1086/657684.

Hall, E.K., Maixner, F., Franklin, O., Daims, H., Richter, A., Battin, T., 2011. Linking microbial and ecosystem ecology using ecological stoichiometry: a synthesis of conceptual and empirical approaches. Ecosystems 14, 261–273.

Hedin, L.O., von Fischer, J.C., Ostrom, N.E., Kennedy, B.P., Brown, M.G., Robertson, G. P., 1998. Thermodynamic constraints on nitrogen transformations and other biogeochemical processes at soil-stream interfaces. Ecology 79 (2), 684–703.

Heijnen, J.J., van Dijken, J.P., 1992. In search of a thermodynamic description of biomass yields for the chemotrophic growth of microorganisms. Biotechnol. Bioeng. 39 (8), 833–858.

Henze, M., Gujer, W., Mino, T., van Loosdrecht, M.C.M., 2000. Activated Sludge Models ASM1, ASM2, ASM2d and ASM3. International Water Association Scientific and Technical Report Series, London.

Huizinga, D., Kolawa, A., 2007. Automated Defect Prevention: Best Practices in Software Management. Wiley-IEEE Computer Society Press, Hoboken, New Jersey, USA.

Izurieta, C., Poole, G.C., Payn, R.A., Griffith, I., Nix, R., Helton, A.M., Bernhardt, E.S., Burgin, A.J., 2012. Development and application of a simulation environment (NEO) for integrating empirical and computational investigations of system-level complexity. Proc. Int. Conf. Inf. Sci. Appl doi:http://dx.doi.org/10.1109/ICISA2012.6220928.

Jørgensen, S.E., Patten, B.C., Straškraba, M., 1992. Ecosystems emerging: toward an ecology of complex systems in a complex future. Ecol. Model. 62, 1–27.

Jørgensen, S.E., Patten, B.C., Straškraba, M., 1999. Ecosystems emerging: 3. openness. Ecol. Model. 117, 41–64.

Jørgensen, S.E., Patten, B.C., Straškraba, M., 2000. Ecosystems emerging: 4. growth. Ecol. Model. 126 (2–3), 249–284.

Jessup, C.M., Kassen, R., Forde, S.E., Kerr, B., Buckling, A., Rainey, P.B., Bohannan, B.J. M., 2004. Big questions, small worlds: microbial model systems in ecology. Trends Ecol. Evol. 19 (4), 189–197.

Jin, Q., Bethke, C., 2003. A new rate law describing microbial respiration. Appl. Environ. Microbiol. 2340–2348. doi:http://dx.doi.org/10.1128/AEM.69.4.

Kalyuzhnyi, S.V., Fedorovich, V.V., 1998. Mathematical modelling of competition between sulphate reduction and methanogenesis in aerobic reactors. Bioresour. Technol. 65, 227–242.

Madigan, M.T., Martinko, J.M., Parker, J., 2003. Brock Biology of Microorganisms, 10th ed. Pearson Education, Inc., Upper Saddle River, NJ, USA.

Menkel, F., Knights, A.J., 1995. A biological approach on modelling a variable biomass yield. Process Biochem. 30 (6), 485–495.

Milly, P.C.D., Betancourt, J., Falkenmark, M., Hirsch, R.M., Zbigniew, W., Lettenmaier, D.P., Stouffer, R.J., 2008. Stationarity is dead: whither water management? Science 319, 573–574.

Myrold, D.D., 1998. Transformations of nitrogen. In: Sylvia, D.M., Fuhrmann, J.J., Hartel, P.G., Zuberer, D.A. (Eds.), Principles and Applications of Soil Microbiology. Prentice-Hall Inc., Upper Saddle River, NJ, USA, pp. 259–294.

Patten, B.C., Straškraba, M., Jørgensen, S.E., 1997. Ecosystems emerging: 1. conservation. Ecol. Model. 96, 221–284.

Peil, K.M., Gaudy Jr., A.F., 1971. Kinetic constants for aerobic growth of microbial populations selected with various single compounds and with municipal wastes. Appl. Microbiol. 21 (2), 253–256.

Poff, N.L., Brinson, M.M., Day Jr., J.W., 2002. Aquatic ecosystems and global climate change. Pew Research Center, Washington, D.C.

Prosser, J.I., et al., 2007. The role of ecological theory in microbial ecology. Nat. Rev. Microbiol. 5 (5), 384–392.

R. Core Team, 2012. R: a language and environment for statistical computing. R Foundation for Statistical Computing, Vienna, Austria ISBN 3-900051-07-0.

Redfield, A.C., 1958. The biological control of chemical factors in the environment. Am. Sci. 46 (3), 205–221.

Ribot, M., von Schiller, D., Peipoch, M., Sabater, F., Grimm, N.B., Martí, E., 2013. Influence of nitrate and ammonium availability on uptake kinetics of stream biofilms. Freshw. Sci. 32 (4), 1155–1167. doi:http://dx.doi.org/10.1899/12-209.1.

Schneider, E.D., Kay, J.J., 1994. Complexity and thermodynamics: towards a new ecology. Futures 26 (6), 626–647.

Schrödinger, E., 1944. What is Life? Cambridge University Press, Cambridge, UK.

Servais, P., Billen, G., Rego, J.V., 1985. Rate of bacterial mortality in aquatic environments. Appl. Environ. Microbiol. 49 (6), 1448–1454.

Singh, B.K., Bardgett, R.D., Smith, P., Reay, D.S., 2010. Microorganisms and climate change: terrestrial feedbacks and mitigation options. Nat. Rev. Microbiol. 8 (11), 779–790.

Stone, L., Weisburd, R.S., 1992. Positive feedback in aquatic ecosystems. Trends Ecol. Evol. 7 (8), 263–267.

Straškraba, M., Jørgensen, S.E., Patten, B.C., 1999. Ecosystems emerging: 2. dissipation. Ecol. Model. 117, 3–39.

Stumm, W., Morgan, J.J., 1996. Chemical Equilibria and Rates Natural Waters, 3rd ed. John Wiley & Sons, New York.

Tesoriero, A.J., Liebscher, H., Cox, S.E., 2000. Mechanism and rate of denitrification in an agricultural watershed: electron and mass balance along groundwater flow paths. Water Resour. Res. 36 (6), 1545–1559. doi:http://dx.doi.org/10.1029/2000WR900035.

Tijhuis, L., van Loosdrecht, M.C.M., Heijnen, J.J., 1993. A thermodynamically based correlation for maintenance gibbs energy requirements in aerobic and anaerobic chemotrophic growth. Biotechnol. Bioeng. 42, 509–519.

Treseder, K.K., et al., 2012. Integrating microbial ecology into ecosystem models: challenges and priorities. Biogeochemistry 109 (1–3), 7–18. doi:http://dx.doi.org/10.1007/s10533-011-9636-5.

van Loosdrecht, M.C.M., Henze, M., 1999. Maintenance, endogeneous respiration, lysis, decay and predation. Water Sci. Technol. 39 (1), 107–117.

van de Leemput, I.A., Veraart, A.J., Dakos, V., de Klein, J.J.M., Strous, M., Scheffer, M., 2011. Predicting microbial nitrogen pathways from basic principles. Environ. Microbiol. 13, 1477–1487.

Vallino, J.J., Hopkinson, C.S., Hobbie, J.E., 1996. Modeling bacterial utilization of dissolved organic matter: optimization replaces Monod growth kinetics. Limnol. Oceanogr. 41 (8), 1591–1609.

Vallino, J.J., 2010. Ecosystem biogeochemistry considered as a distributed metabolic network ordered by maximum entropy production. Philos. Trans. R. Soc. Lond. B Biol. Sci. 365 (1545), 1417–1427. doi:http://dx.doi.org/10.1098/rstb.2009.0272.

Zarnetske, J.P., Haggerty, R., Wondzell, S.M., Baker, M.A., 2011. Labile dissolved organic carbon supply limits hyporheic denitrification. J. Geophys. Res. 116 (G4) doi:http://dx.doi.org/10.1029/2011JG001730.